Scalable hollow fiber pulse compressor for NIR and UV lasers

Martin Maurel, Matthieu Chafer, Benoît Debord, Foued Amrani, Benoît Beaudou, Frédéric Gérôme, Fetah Benabid

Scalable hollow fiber pulse compressor for NIR and UV lasers

Martin Maurel[a,b],Matthieu Chafer[a,b], Benoit Debord[a,b], Foued Amrani[a], Benoit Beaudou[b], Frédéric Gérôme[a,b], Fetah Benabid*[a,b]

[a]GPPMM group, XLIM CNRS UMR7252, Université de Limoges, Limoges, France;
[b]GLOphotonics SAS, Limoges, France

ABSTRACT

We report on several ultra-short pulse compression schemes based on hollow-core photonic crystal fiber filled with a chosen gas-phase medium and undertaken in a versatile module coined "FastLas". The scheme relies on dispersion management by both fiber design and gas pressure management to offer a highly versatile pulse compressor. Furthermore, the gas is also used to set the required optical nonlinearity. This type of hollow fiber based compressor is scalable with the laser wavelength, pulse energy and initial pulse-width. Among the achieved pulse compression, we list a self-compression of 500-600 fs ultra-short pulse Yb-laser and with energy range of 10-500 µJ. By simply scaling the fiber length we demonstrated pulses as short as ~20 fs for the whole energy range. Here, the self-compression is achieved through solitonic dynamic. Conversely, we demonstrated pulse compression based on self-phase modulation by adjusting the fiber and gas dispersion. Among the pulse compressors we have developed, based on self-phase modulation, we cite the compression of a frequency-tripled micro-Joule pulse-energy Yb-laser with a pulse width of 250 fs. The results show compressed UV-pulses with temporal width in the range of 50-60 fs.

Keywords: USP laser, Compression, Soliton, Kagome HC-PCF

1. INTRODUCTION

Over the last two decades, ultra-short pulse (USP) lasers have witnessed a dramatic progress, both in their design and performance on one hand, and in their applications in varied scientific and industrial fields in another hand. The impact of this progress was exemplified by the award of the 2018 Nobel Prize to Gérard Mourou and Donna Strickland for their seminal work on the Chirp Pulse Amplification (CPA) [1], which enabled the development of USP laser with ultra-high peak power and/or energy. Nowadays, commercially available tabletop lasers emitting pulses with duration of hundreds of femtosecond and milli-Joule energy have become a commonplace. Furthermore, this type of USP lasers are available in the most representative wavelengths, such as 800 nm for Ti:Sapph laser, 1µm for Yb-based laser and 1.5 µm for Er-based laser, and their frequency-doubled and tripled versions. USP lasers are now found in a vast number of applications in various and varied fields like surgery, ophthalmology, industrial metal cutting, micro engineering and fundamental research. Within this USP laser landscape, Ytterbium-based laser, with its varied technology (i.e. fiber, thin disk, slab or crystal), outstand with its capacity to fulfill most of the performance specifications. The Yb-based laser offers a superior power-scaling, it can be operated in different operational modes, such as emitting from CW regime to 100 fs pulses with repetition rate from kHz to GHz repetition rate. However, despite a gain bandwidth which can be as large 100 nm, indicating that 20 fs pulse-width could be achievable [2], the typically generated pulses from high energy (>10µJ) Yb-based lasers exhibit duration in the range of 400 fs to 1 ps, and achieving sub-100 fs remains a challenging task despite the implementation of ingenious schemes to overpass this limitation [3]. In turn, this limits their impact in some of the emerging industrial applications where processing of some materials such as dielectric or semiconductor require 10-100 µJ level pulses with pulse-width below 300 fs.

In parallel with USP development, photonics witnessed the advent of hollow-core photonic crystal fiber (HCPCF) whose properties make it potentially a timely booster to further the development of USP lasers and their adoption by the industry. Indeed, HCPCF can be used as an outstanding fiber beam delivery or extremely efficient nonlinear compressor. This is particularly true with hypocycloid core-contour Inhibited-Coupling guiding HCPCF (IC-HCPCF) which combines ultra-low transmission loss, low dispersion, very weak optical overlap between the core mode and the silica cladding [4] [5], [6][7]. Actually, several demonstrations have been reported for both USP laser beam-delivery and pulse compression. For example, USP lasers with pulses in the range of 20-500 fs and energy of up to ~3 mJ have been guided in several meter

long IC-HCPCF [7] [8]. Also, with an adequate cooling fiber mounting, lasers with average power as high as 1 kW was reported [9]. With regard to pulse compression in IC-HCPCF, it was achieved with USP lasers emitting at most of the representative wavelengths. For example, Wang *et al.* reported in 2012 the compression of 1.5μm wavelength, 100 μJ pulse energy, and 850 fs duration from a USP Er-fiber laser down to 300 fs [4]. With Yb-based lasers, the compression via self-phase modulation (SPM) spectral broadening was demonstrated in several instances [8], including with average power as high as 100 W [10]. Also, it was achieved via soliton spectral dynamic [7]. Close to a single-cycle self-compression was reported with 1.8μm wavelength, 80 fs and ~40 μJ USP laser [11]. Finally, SPM broadening was also achieved with milli-Joule level and 20 fs pulses emitted at ~800 nm from Ti-saph USP laser system, indicating a potential compression down to less 10 fs [8].

Whilst beam-delivery based on IC-HCPCF is now commercially available in robust and industrial-grade modules, IC-HCPCF based pulse compressor remains limited to optical laboratory. Several reasons justify such a state-of-affair. The first and main one is the difficulty in defining the performance specifications in a highly evolving field such as that of USP lasers. The second one is the lack of an easy-access to a robust, modular and user-friendly compression module that can be used as a performance test-bed for such a novel pulse compression scheme. Finally, the physics of the optical nonlinear effect that can be excited are sensitive to the IC-HCPCF and filling gas parameters such the mode field diameter and dispersion and the gas nonlinear response.

Here, we report on a pulse compression module-coined FastLas, and available through the company GLOphotonics [12]- that addresses some of the above limitations by allowing the user to adjust in an easy manner the control parameters like the IC-HCPCF design, filling gas and cooling. The compressor relies on dispersion management by both fiber design and gas pressure management to offer a highly versatile pulse compressor. Furthermore, the gas is also used to set the required optical nonlinearity. This type of hollow fiber based compressor is scalable with the initial pulse energy, pulse-width, wavelength and average power. As an illustration, we have used two different IC-HCPCFs to demonstrate pulse compression at two different wavelengths and with two different spectral broadening mechanisms. In the first example, we show self-compression of 500-600 fs ultra-short pulse Yb-laser and with energy range of 10-500 μJ. By simply scaling the fiber length with the input energy, we demonstrated pulses as short as ~20 fs for the whole energy range using a scheme based on air-filled IC-HCPCF with a dispersion profile that favors solitonic dynamic. The second compressor example is based on IC-HCPCF designed to compress via SPM pulses a frequency-tripled micro-Joule pulse-energy Yb-laser with a pulse width of 250 fs. We show compressed UV-pulses with temporal width in the range of 50-60 fs. Finally, the compression module was also tested to operate at high average power whereby SPM broadening and pulse-compression of Yb-based USP laser was achieved with average power as high as 100 W.

2. HC-PCF PROPERTIES AND SET-UP

2.1 FastLas description and experimental set-up

Fig. 1 shows a picture of the FastLas compression module and an example of a typical experimental set-up where to incorporate the compressor. The set-up can be very simple, for it is usually composed by a USP laser to compress, polarizing optics (e.g. a half-waveplate (λ/2) and a polarizing beam splitter (PBS)) to control and monitor the laser power, and beam-steering mirrors (M1 in Fig. 1b) to couple the beam into the FastLas. At the compressor output, the beam is sent for temporal and spectral characterization using beam-steering mirrors. The choice of the latter depends on the structure of the broadened spectrum and its chirp. When the spectral broadening is driven by SPM, we use dispersive mirrors such as Gires-Tournois Interferometer or Group Delay Dispersion (GDD) mirror to both compensate the dispersion for post-compression and to steer the beam (M2 and M3 in Fig. 1b). Given the very low value of the IC-HCPCF dispersion (see section below) and the sub-sequent small chirp of the generated SPM spectrum in low pressure inert gases, one GDD mirror is often sufficient for an efficient compression (see sections below). In the case of pulse self-compression via soliton generation, dispersive optics is often not required [11].

The FastLas is equipped with a purposely designed HCPCF mounted in a hermetically sealed and water-cooled cell for gas management and operation at high average optical power levels respectively. Both functionalities can be easily deployed through gas and water connections. The FastLas is also equipped with a pre-aligned optics for quick and easy coupling into the fiber. This pre-alignment procedure is useful with high energy or high average power lasers because it allows avoiding damaging the HCPCF via misalignment of laser beam with the fiber core.

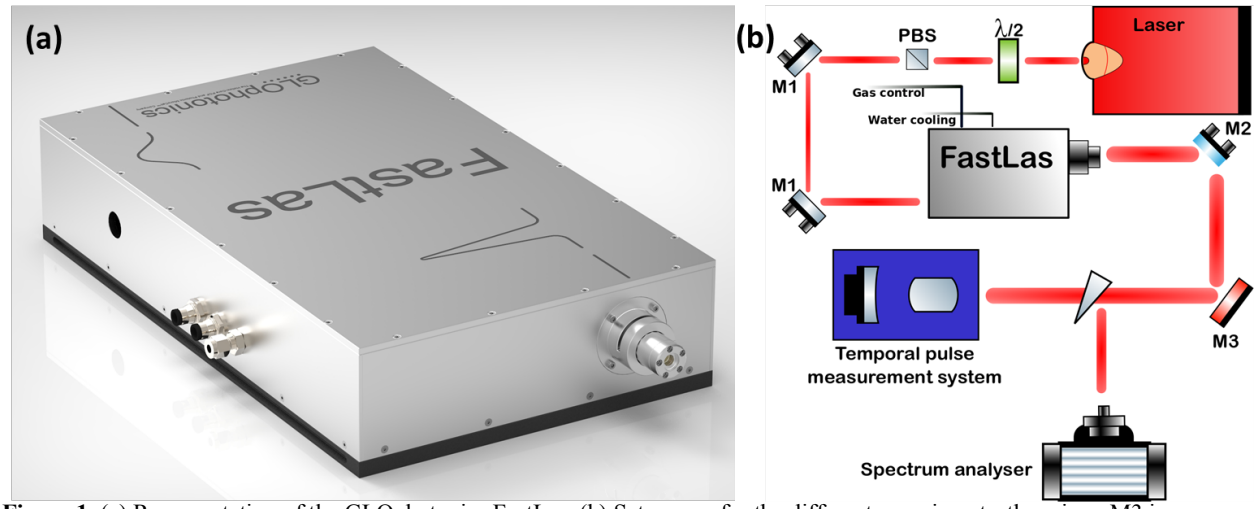

Figure 1. (a) Representation of the GLOphotonics FastLas. (b) Set-up use for the different experiments, the mirror M3 is different each time.

2.2 HCPCF definition and characterization

The fibers used in this work are all based on the same IC optical guidance mechanism, and having a hypocycloid (i.e. negative curvature) core-contour. Fig. 2 shows the micrograph of the two fiber transverse profiles. The first fiber (Fiber #1) has a cladding with Kagome lattice structure (see Fig. 2(a)) [5], and the second one (Fiber #2) exhibits a tubular amorphous lattice cladding (see Fig. 2(b)) [13].

Fiber #1 has an MFD of 42 µm, and Fiber #2 has an MFD of ~29 µm. We have used the two fiber designs to develop two FastLas compressors. Both fibers are manufactured by, and commercially available from GLOphotonics. The first one is optimized to operate at 1 µm wavelength with a loss figure of 30 dB/km. Fiber #2 operates at 343 nm wavelength with a loss figure 500 dB/km. The choice of the two fibers was motivated to cover several specifications from the laser pulse parameter set of (energy, wavelength, duration, average power) on one hand, and to excite two different types of optical nonlinear spectral broadening mechanisms. The first target mechanism is a soliton generation and the second one is SPM.

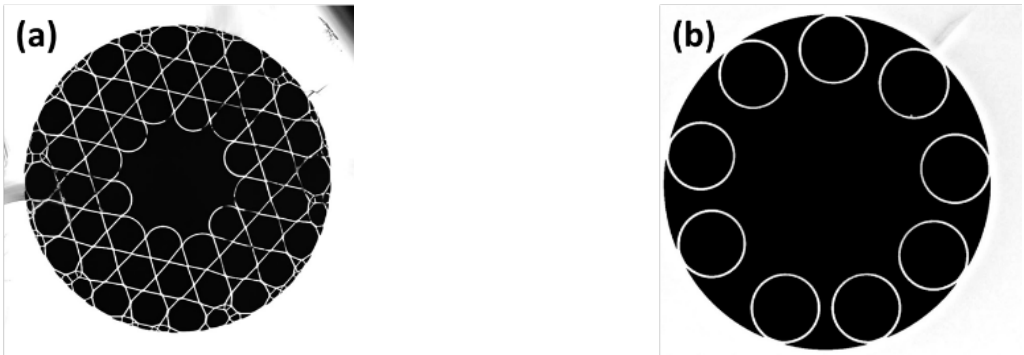

Figure 2 Micrographs of Kagome HCPCF (a) and Tubular amorphous lattice HCPCF (b).

It is noteworthy that the pulse propagation dynamics and nonlinear optical phenomena are very complex and sensitively depend on the aforementioned laser pulse parameter set, on the fiber physical and optical properties (e.g. length, dispersion, mode field diameter) and on the gas dispersion and nonlinear response. Consequently, predicting the spectral and temporal profile of the output pulse in a rigorous manner requires heavy numerical simulations especially for input pulse duration

that are too short to apply the slowly varying approximation, or for too high pulse intensity to properly account of the photo-induced ionization.

Despite such complexity, one can easily define the appropriate fiber parameter-space for pulse compression by delineating a limited number of relevant parameters. For this purpose, we recall that the regime of pulse propagation in a fiber can primarily be defined by the scale of the following lengths: (i) laser-matter interaction effective length, $L_{eff} = (1 - e^{-\alpha L})\alpha^{-1}$, with L being the fiber length and α the transmission loss coefficient, (ii) the dispersion length, $L_D = \tau_p|\beta_2|^{-1}$, with τ_p being the laser pulse-width and β_2 is the group velocity dispersion (GVD) parameter of the guiding medium; and (iii) the nonlinear length, $L_{nl} = (\gamma P_p)^{-1}$, with $\gamma = 2\pi\, n_2 \left(\lambda A_{eff}\right)^{-1}$ being the nonlinearity coefficient, and P_p the peak power of the input laser pulse.

Here, L_{nl} and the L_D respectively provide the required length scales over which the optical nonlinear and dispersive effects become important for a pulse propagating in fiber of length *L*. Consequently, by putting a figure on the magnitude of L_{eff}, L_D and L_{nl} and on the ratios L_{eff}/L_D, L_{eff}/L_{nl} and L_D/L_{nl} on can determine the propagation regime, between that of spectral-temporal distortion free regime from that of linearly dispersive or nonlinear regime, and can estimate the dominant one. For example, in order to have strong optical nonlinear response with little dispersive effect L_{eff}/L_{nl} must be large and L_{eff}/L_D must be small respectively. Furthermore, one can even control the optical nonlinear dynamics by setting the sign of β_2. Indeed, for a spectral range with positive β_2 the optical nonlinearity is dominated by SPM if we consider a medium with no Raman response or resonant parametric wave mixing. On the other hand, for negative β_2, the pulse propagation witnesses soliton formation. We applied this approach in choosing Fiber #1 and Fiber #2.

Table 1 shows the relevant parameters of the designed fibers for the aforementioned purpose. Fiber #1's cladding microstructure and core size were set so its dispersion length at the input laser wavelength L_D is sufficiently long compared to the nonlinear length L_{nl}. Both lengths can be further adjusted by an appropriate choice of gas and its pressure. Here, the non-linear length can be scaled from 0.165 m for 1 bar or Argon to 0.011 m for 15 bar of Argon for the case of a 1030 nm laser pulse of 500 fs duration and 100 μJ energy. Similarly, controlling the gas pressure can significantly change the dispersion length. For example we can more than double L_D by increasing the Argon gas pressure from 1 bar to 15 bar. We note that for the 500 fs pulse duration, L_D is typically in the order of ~ a few meters for a solid core fiber, whilst in Fiber #1 it is up to 3 orders of magnitude longer. Furthermore, the zero dispersion wavelength (ZDW) can also be tuned by changing the gas and its pressure, thus giving further maneuver to operate in the normal or anomalous dispersion.

Fiber	**MFD (μm)**	**Loss (dB/km)**	***1 bar Argon***			***15 bar Argon***		
			L_d **(m)**	**ZDW (nm)**	L_{nl} **(m)**	L_d **(m)**	**ZDW (nm)**	L_{nl} **(m)**
#1	42	30 (@ 1030)	852	790	0.165 (I = $7.07.10^{16}$)	1890	930	0.011 (I = $7.07.10^{16}$)
#2	29.4	500 (@ 343 nm)	473	374	2.202 (I = $2.77.10^{15}$)	71	412	0.146 (I = $2.77.10^{15}$)

Table 1. Summary of the geometrical and optical properties of the fibers used. Intensity calculated for 500 fs and 100 μJ for fiber #1 and 200 fs 1 μJ for fiber #2.

Figure 3(a) illustrates the same GVD scalability with gas pressure control by plotting the GVD and the third order dispersion (TOD) spectra for two Ar gas pressure values. Recalling that Fiber #1 was designed to operate in anomalous dispersion, β_2 was found to be -400 fs^2/m and -190 fs^2/m for 1 and 15 bar respectively, and in accordance with our aim to favor a solitonic dynamics. Figure 3(a) shows also the loss spectrum of the transmission band of interest.

Similarly, Table 1 and figure 3(b) present the same parameters for Fiber #2. Here, the difference is that the Fiber is designed to operate at 343 nm in the normal dispersion regime to excite SPM.

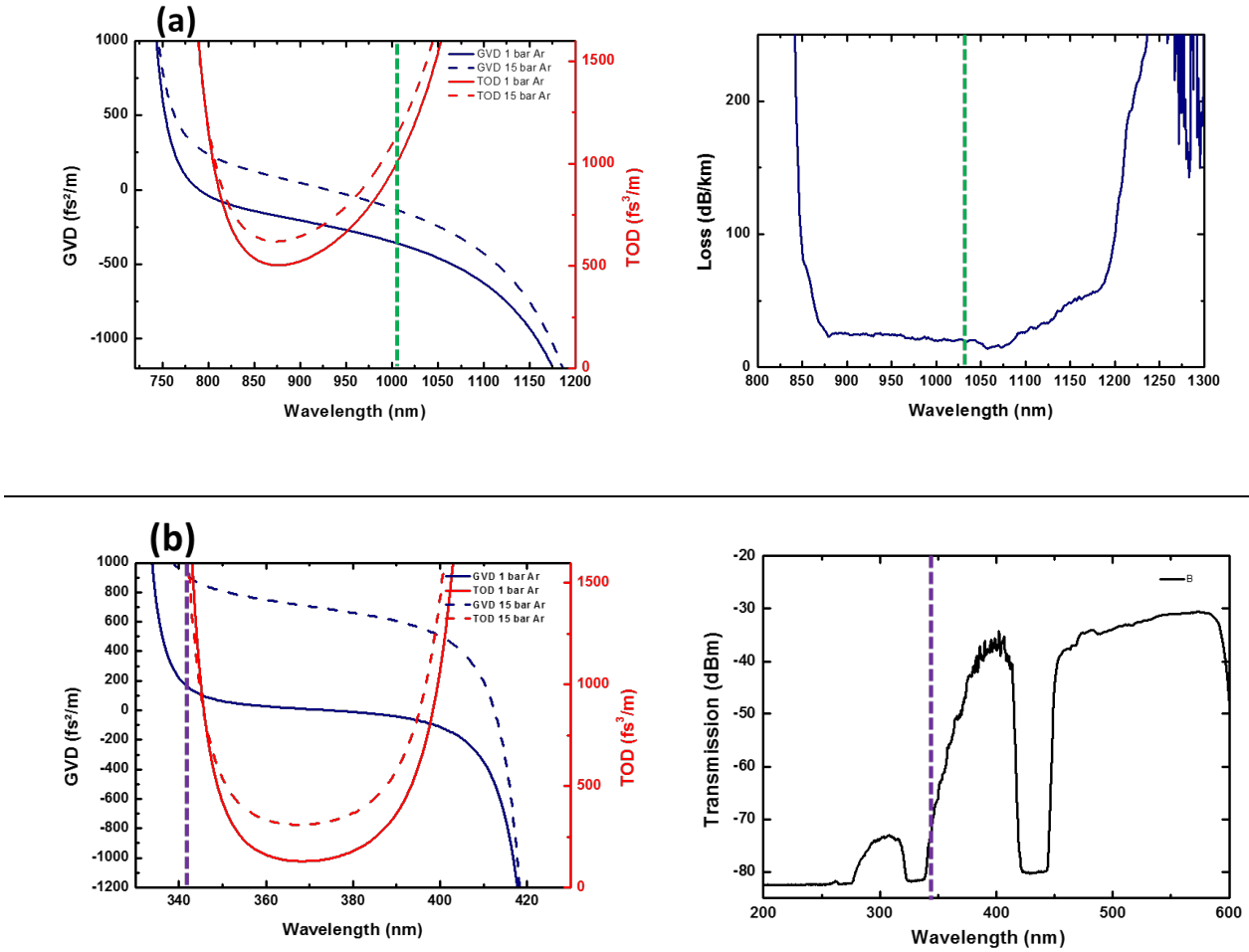

Figure 3 Calculated GVD and TOD (lhs), measured loss and transmission (mhs), micrograph of the two fibers studied (rhs)

3. EXPERIMENTAL RESULTS

3.1 Solitonic compression of 1030 nm wavelength laser pulses

Fiber #1 was used under two gas configurations. The first configuration is based simply keeping the fiber exposed to atmospheric air, representing a GVD of -350 fs²/m at 1030 nm. The second configuration is based on filling the fiber with Argon at 300 mbar.

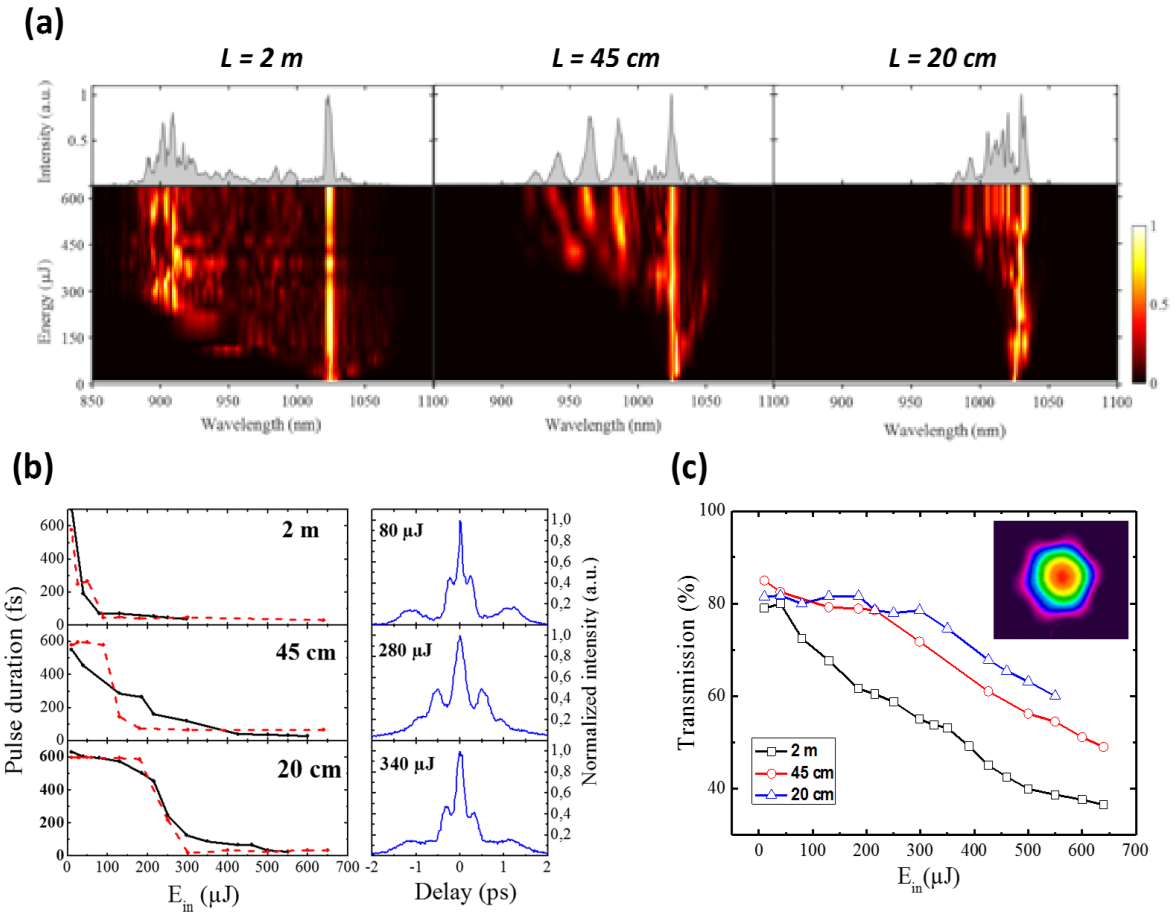

Figure 4. a. Spectral broadening of the experiment for different fibers length. b. Pulse duration evolution with the energy, autocorrelation trace for the fiber length studied. c. Transmission of the fiber regarding the energy.

In the first configuration, the 600 fs duration input laser pulse is emitted from a 1030 nm laser with a repetition rate equal to 1 kHz and a maximum energy of 1 mJ. The laser beam is coupled into the Kagome fiber with transmission coefficient greater than 80%. Different fibers lengths and energy values were explored in recording the output pulse spectral and temporal profiles. Figure 4(a) shows the evolution of the generated and transmitted spectrum with input pulse energy for 3 different representative fiber lengths. The three spectral evolutions show comparable dynamics with the generation of blue-shifted spectral components. The results show that with increasing the fiber length, the onset of the blue-shifted spectrum occurs at smaller energy values, and the frequency-shift increases. At the energy of the onset of the blue-shifted spectrum is associated with a sudden compression (Fig. 4(b)) associated with soliton generation (Fig. 4(b)). The compression is quickly flowed by sideband in its pulse temporal profile indicating soliton fission. The theory show that the observed compression dynamics is driven by an interplay between soliton self-compression and ionization in corroboration with the linear decrease of the transmission coefficient for input pulse energy larger than the energy corresponding to the sudden compression ((Fig. 4(c)).

Despite the sensitivity of such self-compression phenomenon to input pulse energy, the results show that it can be used as energy-scalable and stable pulse-compressor, as illustrated by figure 5. Figure 5(a) shows the fiber-length and input-pulse-energy pairs for optimal compression. Figure 5(b) represents the typical compressed pulse for an optimal pair-value of fiber length and pulse energy. It shows a pulse compression down to 22 fs (red curve) compared to the 600 fs input pulse duration (blue curve), which represents a compression ratio in “single-stage” scheme of close to 30. Furthermore, Figure

5(c) shows the stability of the compressed pulse with time by recording the output pulse frequency resolved optical gating (FROG) spectrogram (insets) regularly over 5 hours.

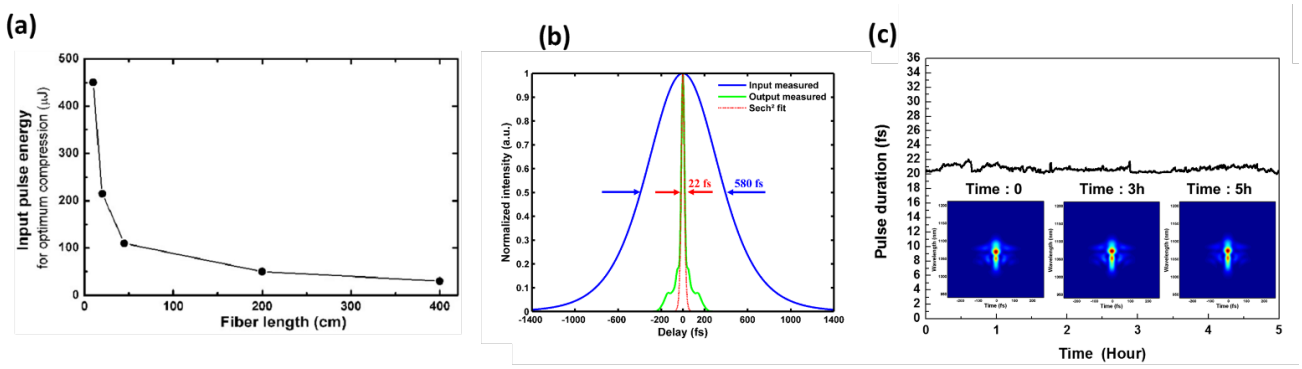

Figure 5. a. Scaling law for the optimal compression. b. Compressed pulse (red curve) compared to the input pulse duration. c. Stability of the pulse compression over 5 hours.

The Fiber #1 and the FastLas technology were tested using a different laser and gas. Here, the laser emits, at 1030 nm wavelength, pulses of 130 fs duration and repetition rate of 166 kHz. The fiber length was set to 1.20 m and was filled with 300 mbar of Argon. Figure 6(a) represents the spectrum and pulse duration at a power of 3 W. The optimal compression down to 30 fs is obtained for a pulse energy of 63 µJ corresponding to 10.4 W presented figure 6(b). In the same way than presented before, this self-compression is associated to an important blue-shift of the pulse spectrum.

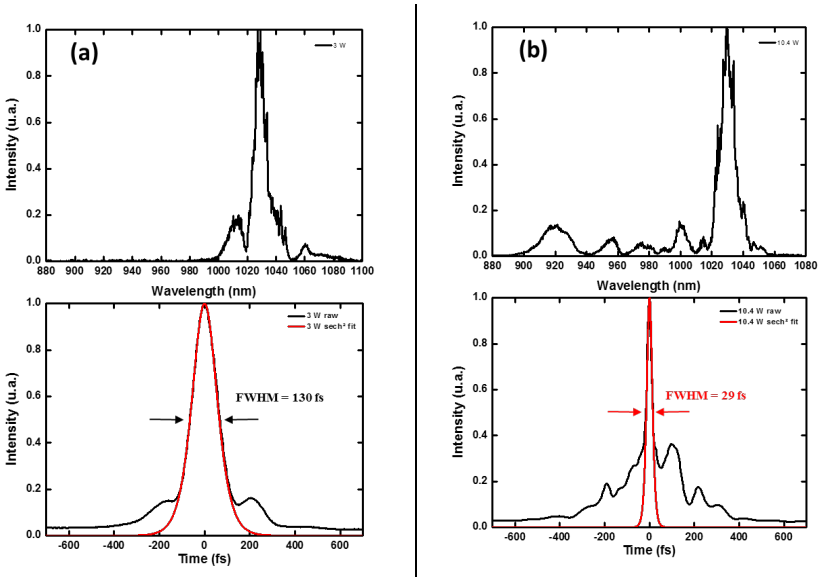

Figure 6. a) Spectrum (top) and temporal profile (bottom) at 3 W after propagation in 1m20 of fiber length filled with 300 mbar of Argon. b) Spectrum (top) and temporal (bottom) profile at 10.4 W after propagation in 1m20 of fiber length filled with 300 mbar of Argon.

3.2 SPM based compression of 434 nm wavelength laser pulses

The set-up comprises a frequency-tripled Yb ultrafast laser emitting unchirped Gaussian pulses with 4.5µJ energy, 250fs duration and 200 kHz repetition rate, and a variable length of fiber #2 integrated in the FastLas platform. As mentioned above, the fiber is purposely designed to have the laser wavelength positioned at a transmission-band blue-edge to ensure normal dispersion for different gas-filling configuration, and subsequently to operate in “SPM regime”.

Figure 7(a) shows the typical measured spectra and autocorrelation traces of the IC-HCPCF-transmitted laser with increasing input energy when the fiber-length and gas-pressure are optimized. Here, the fiber length is 0.7 m and filled with Argon at a pressure of 15 bar. The results show respectively a spectral broadening and temporal narrowing as the laser energy is increased from ~1µJ to ~4 µJ. The spectrum broadens ~20 fold from 3 THz to more than 60 THz, whilst the pulse duration is narrowed from 250 fs to 50 fs. The post-compression is achieved by partially compensating the SPM induced chirp with a dielectric mirror exhibiting negative GVD at the working spectral range. Figure 7(b) summarizes the effect of the fiber length on the pulse compression for air-filled fiber (red curve) and 15bar argon-filled fiber (blue curve). An optimal result is presented figure 7(c) with 0.7 m of fiber filled with 15 bar of argon The results show an optimum length for maximum compression, and occurs at 3.5 m for air-filled and at 0.7 m for 15 bar Argon-filled.
Furthermore, the results show that with the achieved spectral broadening, a compression of the pulse down to less than 5 fs is possible with a full chirp compensation.

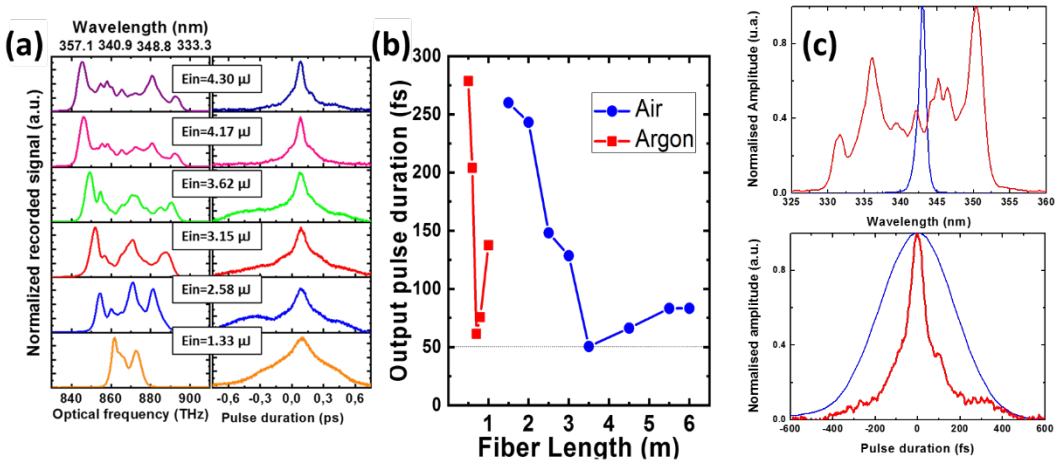

Figure 7.a. Output spectrum (lhs) and temporal trace (rhs) evolution with laser input energy. b. Measured Pulse-width with fiber length for air-filled fiber (blue curve), and 15 bar Ar-filled fiber (red). c. Spectrum of the initial laser pulse (blue curve), the pulse after propagation in 0.7 m long Argon-filled HCPCF as experimentally measured (red curve). d. same as (c) for temporal traces

4. CONCLUSION

In conclusion, we developed an IC-HCPCF based pulse compressor module, coined FastLas. We verified its performance, versatility and scalability by choosing only two different HCPCF to demonstrate nonlinear compression with different pulse wavelengths, durations and energies. Among the presented results, we listed the self-compression of 600 fs pulses emitted from 1030 nm wavelength laser down to 22 fs, and of 130 fs from 1030 nm wavelength high average power laser down to ~30 fs using solitonic dynamics. Also, we have demonstrated SPM based nonlinear compression of 250 fs pulses emitted from 343 nm wavelength laser down to 50 fs, with the potential of further compression down to ~5 fs is the dispersion is fully compensated.

ACKNOLEDGMENTS

The authors are grateful to C. Valentin and Y.xxxx (add the name of the people involved) from the CELIA UMR5107 for the help on one of the presented experiments.

REFERENCES

[1] D. Strickland and G. Mourou, “Compression of amplified chirped optical pulses,” *Opt. Commun.*, vol. 55, no. 6, pp. 447–449, Oct. 1985.

[2] D. J. Richardson, J. Nilsson, and W. A. Clarkson, “High power fiber lasers: current status and future perspectives [Invited],” *J. Opt. Soc. Am. B*, vol. 27, no. 11, p. B63, Nov. 2010.
[3] J. Pouysegur *et al.*, “Numerical and experimental analysis of nonlinear regenerative amplifiers overcoming the gain bandwidth limitation,” *IEEE J. Sel. Top. Quantum Electron. Inst. Electr. Electron. Eng.*, vol. 21, no. 1, 2015.
[4] Y. Y. Wang *et al.*, “Design and fabrication of hollow-core photonic crystal fibers for high-power ultrashort pulse transportation and pulse compression,” *Opt. Lett.*, vol. 37, no. 15, p. 3111, 2012.
[5] B. Debord *et al.*, “Hypocycloid-shaped hollow-core photonic crystal fiber Part I: Arc curvature effect on confinement loss,” *Opt. Express*, 2013.
[6] M. Alharbi *et al.*, “Hypocycloid-shaped hollow-core photonic crystal fiber Part II: Cladding effect on confinement and bend loss,” *Opt. Express*, 2013.
[7] B. Debord *et al.*, “Multi-meter fiber-delivery and pulse self-compression of milli-Joule femtosecond laser and fiber-aided laser-micromachining,” *Opt. Express*, vol. 22, no. 9, p. 10735, May 2014.
[8] B. Debord, F. Gérôme, P.-M. Paul, A. Husakou, and F. Benabid, “2.6 mJ energy and 81 GW peak power femtosecond laser-pulse delivery and spectral broadening in inhibited coupling Kagome fiber,” in *CLEO: 2015*, 2015, p. STh4L.7.
[9] S. Hädrich *et al.*, “Scalability of components for kW-level average power few-cycle lasers,” *Appl. Opt.*, vol. 55, no. 7, p. 1636, Mar. 2016.
[10] F. Emaury *et al.*, “Efficient spectral broadening in the 100-W average power regime using gas-filled kagome HC-PCF and pulse compression,” *Opt. Lett.*, 2014.
[11] T. Balciunas *et al.*, “A strong-field driver in the single-cycle regime based on self-compression in a kagome fibre,” *Nat. Commun.*, vol. 6, no. May 2014, pp. 1–7, 2015.
[12] “Home - Glophotonics.” [Online]. Available: http://www.glophotonics.fr/. [Accessed: 15-Jan-2019].
[13] B. Debord *et al.*, “Ultralow transmission loss in inhibited-coupling guiding hollow fibers,” 2017.